

## 2.60

# Mixed Valence Dinuclear Species

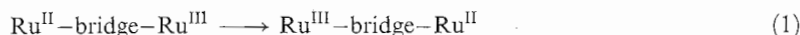
J. T. HUPP

*Northwestern University, Evanston IL, USA*

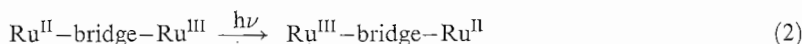
2.60.1	INTRODUCTION	709
2.60.2	EARLY EXPERIMENTS: APPARENT EVIDENCE FOR VALENCE LOCALIZATION	711
2.60.3	EVIDENCE FOR VALENCE DELOCALIZATION	711
2.60.4	BORDERLINE BEHAVIOR	711
2.60.5	DELOCALIZATION MECHANISM	712
2.60.5.1	Theory	712
2.60.5.2	Experiment	714
2.60.6	DETAILED ELECTRONIC STRUCTURE	715
2.60.7	ANOTHER PERSPECTIVE	715
2.60.8	REFERENCES	716

### 2.60.1 INTRODUCTION

The Creutz-Taube ion,  $(\text{NH}_3)_5\text{Ru}(\mu\text{-pyrazine})\text{Ru}(\text{NH}_3)_5^{5+}$ , was one of the earliest intentionally prepared molecular mixed-valence complexes.<sup>1,2</sup> Initially formulated as  $\text{Ru}^{\text{II}}$ -bridge- $\text{Ru}^{\text{III}}$ , it was intended by its designers to provide an example of the direct experimental assessment of the reorganization energy for an intramolecular electron transfer reaction—in this case:



Briefly, the idea was to use Hush's theory relating optical intervalence transfer (Equation (2)) to thermal electron transfer (Equation (1)).<sup>3</sup> As summarized in Figure 1 for a symmetrical system



an electronic absorption is expected at an optical energy equaling the total reorganization energy, and also equaling four times the activation free energy for nonadiabatic electron transfer. Hush had previously shown that the theory could be applied to mixed-valent mineral compounds, with optical intervalence transitions accounting in many cases for the colors of the minerals.<sup>4</sup> Before Creutz and Taube's report, however, the theory hadn't been applied to well-defined symmetrical molecular systems in solution environments.

As shown in Figure 2, the Creutz-Taube (CT) ion yields the intervalence absorption band promised by Hush theory.<sup>1,2</sup> Furthermore, the band appears at an energy that seems reasonable as an electron-transfer reorganization energy. In other respects, however, the observations are inconsistent with the Hush model. Most notably, the band is non-gaussian and is much narrower than expected from the model (which relates the width to the reorganization energy). Furthermore, it is relatively insensitive to solvent composition, with a residual sensitivity that differs from what is expected from solvent contributions to the reorganization energy. The observations were considered particularly striking in view of the closely related compound,  $(\text{NH}_3)_5\text{Ru}(\mu\text{-4,$

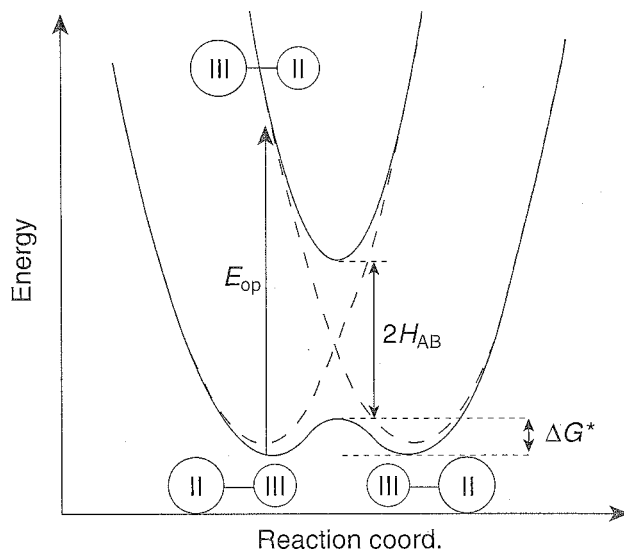


**Figure 1** Hush diagram for intervalence transfer within a class II mixed-valence ion. The dotted lines correspond to diabatic potential energy surfaces. The solid lines are adiabatic potential energy surfaces. Electron transfer can occur either optically (vertical transition with energy,  $E_{op}$ , equaling  $\lambda$ ) or thermally by moving along the lower adiabatic surface. In the diabatic limit, the barrier height for thermal electron transfer is  $\lambda/4$ .

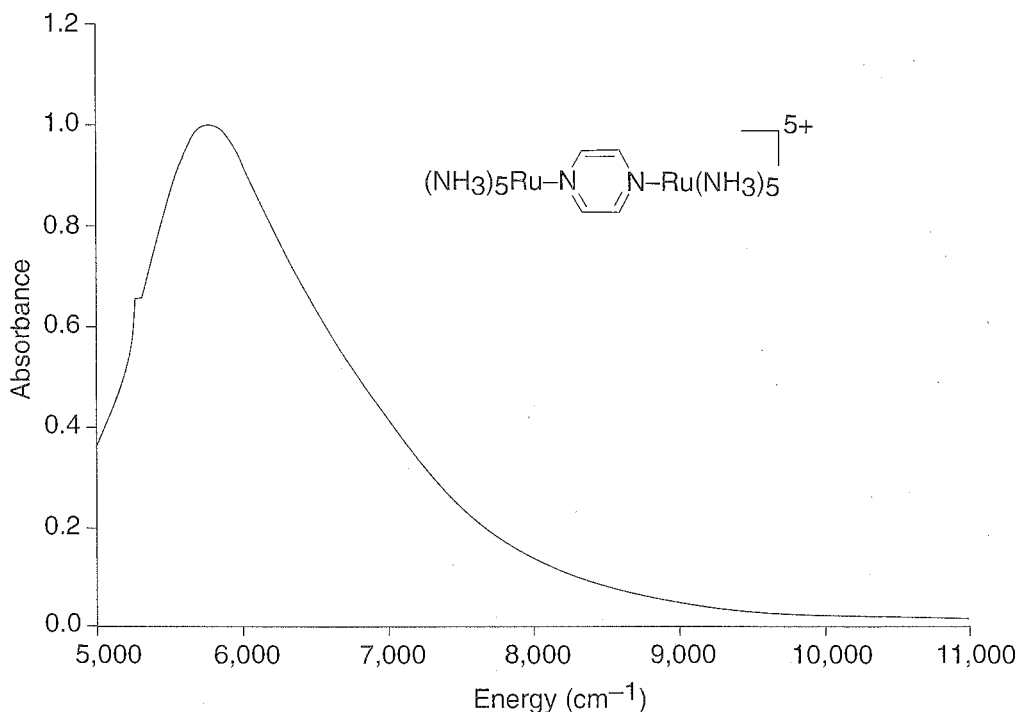


**Figure 2** Electronic absorption spectrum of the Creutz-Taube ion in the intervalence region, in nitromethane as solvent.

4'-bipyridine) $\text{Ru}(\text{NH}_3)_5^{5+}$ .<sup>5</sup> In contrast to the CT ion, this compound displays a broad gaussian intervalence band that varies in energy according to the optical and static dielectric properties of the solvent, as expected from Marcus-Hush theory.<sup>3,6</sup>

The disparate observations suggested an alternative formulation of the CT ion as a valence-delocalized compound, i.e.,  $\text{Ru}^{\text{III}/2}\text{-bridge-Ru}^{\text{III}/2}$ , where the delocalization is an intrinsic electronic

property, not a dynamical timescale or hopping-rate related effect.<sup>7</sup> The question of localization versus delocalization turned out to be something of a challenge to answer. A large number of ingenious analyses were applied in the years following the initial report in 1969 of the ion's synthesis. Something of a consensus (in favor of delocalization) was finally reached around 1984.<sup>8</sup> At about the same time, theorists began to consider and debate competing ideas concerning the *mechanism* of delocalization.<sup>9-12</sup> Definitive experimental evidence in support of one of the mechanisms was finally obtained in 1994.<sup>13</sup>

### 2.60.2 EARLY EXPERIMENTS: APPARENT EVIDENCE FOR VALENCE LOCALIZATION

Several early experiments purporting to show valence localization were subsequently found to be artifactual (due to photo decomposition, contamination, and other problems). Others reported sound observations, but their interpretation proved to be more subtle than initially appreciated. For example, XPS measurements of the CT ion yielded two Ru peaks, seemingly indicating that atoms in two distinct oxidation states are present.<sup>14</sup> Hush and co-workers showed, however, that the high polarizability of the CT ion could lead to a splitting of the photoionized valence state of the delocalized complex and, therefore, two XPS peaks.<sup>7,15</sup>

### 2.60.3 EVIDENCE FOR VALENCE DELOCALIZATION

In 1984 six research groups pooled their expertise to study the CT ion.<sup>8</sup> Based on several experimental observations, including the following, they concluded that the ground-state complex exists in delocalized form: (i) X-ray crystallographic studies yielded identical metal-ligand bond lengths for the two metal centers. In contrast,  $(\text{NH}_3)_5\text{Ru}^{\text{II}}(\text{pyrazine-CH}_3)^{3+}$  and  $(\text{NH}_3)_5\text{Ru}^{\text{III}}(\text{pyrazine-CH}_3)^{4+}$  display Ru—N(pyrazine) bond lengths that differ by 0.13 Å.<sup>16</sup> (ii) <sup>99</sup>Ru Mössbauer measurements showed one quadrupole-split doublet peak, instead of the pair of peaks expected from a superposition  $\text{Ru}^{\text{II}}$  and  $\text{Ru}^{\text{III}}$  spectra. These results are consistent either with intrinsic delocalization or with detrapping (i.e., electron exchange within an intrinsically localized state, but on a time scale that is fast compared with the time scale sampled by the probe measurement). (iii) Polarized single-crystal ESR measurements that were not inconsistent with delocalization. (iv) Spectroelectrochemical measurements in the IR region showing a single  $\text{NH}_3$  bend, rather than the pair expected from the simultaneous presence of  $\text{Ru}^{\text{II}}$  and  $\text{Ru}^{\text{III}}$  centers.<sup>17</sup> Similar observations have been reported by Beattie and co-workers for other regions of the IR spectrum.<sup>7</sup> Again, however, detrapping on the IR timescale could provide an alternative explanation. (Several examples of detrapping on the IR timescale have been reported by Meyer and co-workers,<sup>18</sup> as well as Kubiak and co-workers.<sup>19</sup>) More telling is the near absence of IR intensity for an asymmetric stretch of the pyrazine bridge. This band is readily observed in a valence-localized analog of the CT ion,  $(\text{bpy})_2\text{ClRu}(\mu\text{-pyrazine})\text{RuCl}(\text{bpy})_2^{3+}$ .<sup>20</sup>

The conclusions of the six groups were reinforced in an interesting way by Curtis and co-workers who examined a series of CT-ion derivatives (*trans*-(ligand) $(\text{NH}_3)_4\text{Ru}(\mu\text{-pyrazine})\text{Ru}(\text{NH}_3)_5^{5+}$  species) electrochemically.<sup>21</sup> They found that ligand-induced changes in formal potential at one ruthenium center induced a nearly identical shift in formal potential at the second ruthenium center where no change in coordination environment had been introduced. They concluded that electrons were added and removed from a fully delocalized orbital spanning both metal centers.

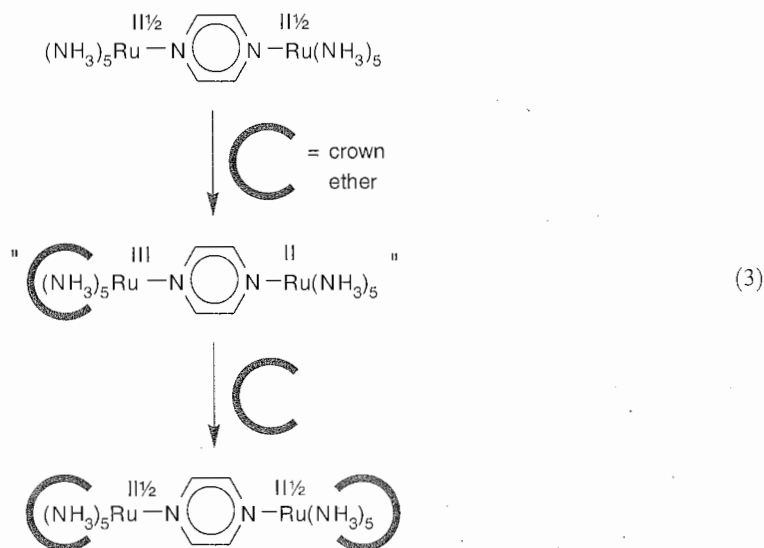
Electronic Stark effect studies by Oh and co-workers revealed that intervalence absorption by the CT ion is accompanied by essentially zero change in dipole moment and, therefore, zero metal-to-metal charge transfer.<sup>22,23</sup> The observations are consistent with a description of the complex as fully delocalized in both the ground state and intervalence excited state. At the same time, the researchers found that intervalence excitation of  $(\text{NH}_3)_5\text{Ru}(\mu\text{-4,4'-bipyridine})\text{Ru}(\text{NH}_3)_5^{5+}$  is accompanied by a large change in dipole moment and, therefore, substantial transfer of charge between metal centers, consistent with a valence-localized description.

### 2.60.4 BORDERLINE BEHAVIOR

In a conventional two-state electronic description, complete valence delocalization occurs when twice the electronic coupling energy ( $H_{\text{ab}}$ ) exceeds the total trapping energy (i.e., the reorganization

energy plus any redox asymmetry). While the experiments described above indicate that the CT ion is fully valence delocalized, additional experiments suggest that the delocalization energy is only marginally greater than the trapping energy. The evidence comes chiefly from experiments in which the symmetry of the system is reduced, thereby increasing the trapping energy. For example, the *trans*-(ligand)(NH<sub>3</sub>)<sub>4</sub>Ru( $\mu$ -pyrazine)Ru(NH<sub>3</sub>)<sub>5</sub><sup>5+</sup> species studied by Curtis and co-workers display broader and more nearly gaussian intervalence absorption line shapes, implying less strong delocalization.<sup>21</sup> Furthermore, the breadth of the intervalence band scales essentially linearly with the magnitude of the introduced redox asymmetry—although in none of the cases examined by these authors does the width reach that expected from Hush's theory for a valence-localized assembly.<sup>4</sup>

A similar but more subtle perturbation has been described by Dong and co-workers.<sup>24</sup> Briefly, they observed that ammine-based hydrogen bonding effects could be exploited to achieve stepwise encapsulation of the two available (NH<sub>3</sub>)<sub>5</sub>Ru sites with large crown ethers. When only one site is encapsulated, the intervalence absorption band is broadened and blue shifted, and acquires a more symmetrical shape. When both are encapsulated, the original line shape is largely restored. From electrochemical studies of monometallic analogs, the redox asymmetry introduced by encapsulating only one of the two available sites can be as large as ca. 0.3 eV. The corresponding spectral effects can be interpreted as manifestations of a polarization effect that, in the extreme, would correspond to valence localization, as shown schematically in Equation (3). Double encapsulation eliminates the redox asymmetry.



Resonance Raman spectroscopy studies show that both kinds of perturbations introduce substantial vibrational complexity; many more modes are coupled to the intervalence transition when the symmetry is reduced and the system is pushed in the direction of valence localization.<sup>25</sup>

## 2.60.5 DELOCALIZATION MECHANISM

### 2.60.5.1 Theory

According to Marcus-Hush theory<sup>3,4,6</sup> and similar two-state treatments, valence delocalization within symmetrical mixed-valence systems occurs when  $2H_{ab}$  exceeds the reorganization energy,  $\lambda$ . Notably, the role played by the bridging ligand is to facilitate orbital mixing and initial-state/final-state coupling in an indirect or super-exchange sense, i.e., by providing virtual intermediate states featuring ligand-localized electrons or holes.<sup>26</sup> In the super-exchange treatment, the lower lying the virtual state, the greater the magnitude of the electronic coupling. For pyrazine-bridged ruthenium complexes,  $\pi^*$  virtual states (electron transfer) are expected to be more important than  $\pi$  virtual states (hole transfer), reflecting the closer energetic proximity of the former to the  $d\pi(\text{Ru})$  donor and acceptor orbitals.

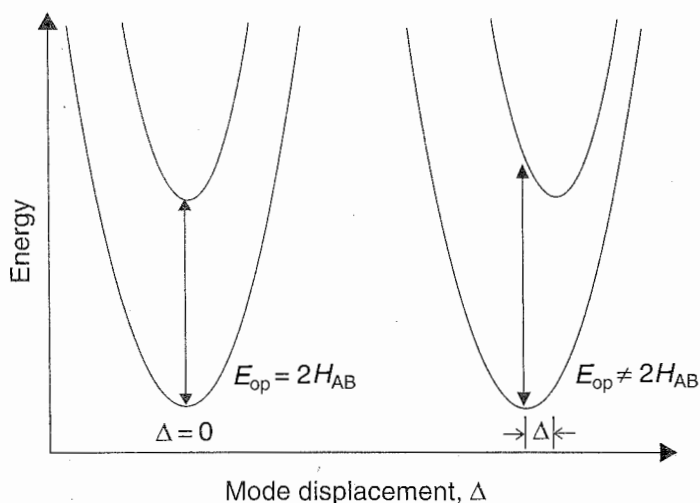


**Figure 3** Potential energy surfaces for class III mixed-valence ions according to the two-state (left-hand side) and three-state (right-hand side) descriptions. In the two-state case, but not the three-state case, the energy of the delocalized “intervalence” transition equals  $2H_{ab}$ . Only in the three-state case are nonzero normal-mode displacements ( $\Delta$ ) encountered.

Piepho, Krausz, and Schatz (PKS) developed a two-state model that recognizes that, in the strong coupling limit, vibrational and electronic excitation may not be entirely separable processes.<sup>9</sup>

In two-state treatments (including Marcus–Hush–Mulliken and PKS), when  $H_{ab}$  is great enough to induce delocalization, the familiar isoenergetic initial and final electronic states (left- and right-hand diabatic states in Figure 1) are replaced with single-welled lower and upper states (nominal one-electron bonding and antibonding states). The energy difference between the states at the well minima is  $2H_{ab}$ . More generally, the energy difference equals  $(\lambda(\Delta q)^2 + 4H_{ab}^2)^{1/2}$ , where  $\Delta q$  is the amount of charge transferred upon intervalence excitation (zero in the case of a symmetrical class III system).<sup>27</sup> As shown in Figure 3 (left-hand panel), for a two-state delocalized system no mode displacement occurs upon intervalence excitation. Under these conditions, the only source of breadth for the absorption band, beyond inhomogeneous broadening, is a change in normal-mode frequency or force constant, manifest in the figure as a different degree of curvature for the upper versus lower surface. Importantly, the modes defining these surfaces are exclusively non-totally symmetric modes. From symmetry considerations, totally symmetric modes can't couple to an intervalence transition in a two-state description.

Two-state models—and the PKS model in particular—do a reasonable job of describing the intervalence absorption spectrum of the CT ion, but fail to capture the spectrum's solvent dependence. A model that does better, as described below, is a three-site/three-state model developed by Ondrechen and co-workers.<sup>10,11</sup> Briefly, rather than viewing bridging ligand orbitals as electronic participants only in a virtual or super-exchange sense, the model incorporates them explicitly in a real sense. In its simplest form, the model combines a  $d\pi_{xz}$  orbital from each ruthenium atom ( $z$  defines the metal–bridge–metal axis) with a pyrazine  $\pi^*$  orbital to create three new orbitals that are formally bonding, nonbonding, and antibonding with respect to the ligand and two metal centers; see Figure 4. Of the three electrons available from the parent Ru orbitals, two occupy the bonding orbital and one half-occupies the nonbonding orbital. The intervalence transition corresponds to promotion of an electron from the three-center (metal–ligand–metal) bonding orbital to the two-center (metal–metal) nonbonding orbital. Thus, the transition has significant ligand-to-metal charge transfer (LMCT) character. Because the charge is symmetrically redistributed to both metal centers, however, there is no change in dipole moment—consistent with Stark measurements. Instead, the ion experiences a change in quadrupole moment.

Further work by Piepho (computational studies) indicates that in addition to a pyrazine  $\pi^*$  orbital, pyrazine  $\pi$  orbitals also likely participate<sup>12</sup>—a point also emphasized by Chou and Creutz.<sup>28</sup> In contrast to two-state models, both the Piepho and Ondrechen models permit coupling of totally symmetric vibrational modes to the intervalence transition, but preclude coupling of non-totally symmetric modes. As shown schematically in Figure 3 (right-hand panel),

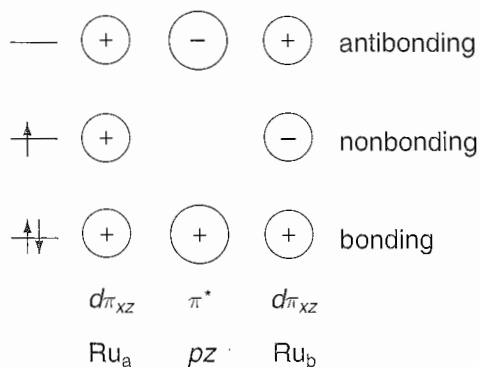


**Figure 4** Qualitative three-state orbital diagram for the Creutz-Taube ion. The combination of two  $d\pi_{xz}(\text{Ru})$  orbitals and one  $\pi^*(\text{pyrazine})$  orbital yields three-center bonding and antibonding molecular orbitals, and a two-center nonbonding orbital. In this model, the intervalence transition at ca.  $5,800\text{ cm}^{-1}$  corresponds to promotion of an electron from the bonding orbital to the nonbonding orbital.

intervalence excitation, in the context of a three-site/three-state model, entails displacement of normal modes.

### 2.60.5.2 Experiment

Among the experimental observations seemingly favoring a three-site/three-state delocalization mechanism over a two-site mechanism is the solvent dependence of the intervalence band energy. The two-state model predicts a dependence upon solvent dielectric properties if the system is localized, but no variation with solvent if the system is delocalized. Instead the energy is invariant and is equal to  $2H_{ab}$ . In contrast, experimental measurements show that the band energy is very weakly solvent dependent. Furthermore, the residual solvent dependence does not correlate with dielectric properties. Instead, a correlation exists with the potential for the  $\text{CT}^{5+/4+}$  redox couple. Ammine complexes typically exhibit strongly solvent-dependent redox potentials. The origin of the solvent dependence is in hydrogen bonding between ammine protons and solvent molecules, where changing the oxidation state of the metal center substantially affects the H-bonding capability of the amines.

What about the three-state model? As Creutz and Chou have pointed out, here the salient feature is the energy gap between the  $d\pi(\text{Ru})$  and  $\pi^*(\text{pyrazine})$  orbitals used to generate the three-center bonding and two-center nonbonding orbitals of the delocalized mixed-valence ion.<sup>28</sup> By taking advantage of ammine-ligand/solvent H-bonding interactions, they were able to show in a series of electrochemical experiments that solvent variations could alter the energy of the  $d\pi(\text{Ru})$  orbital while leaving the pyrazine  $\pi^*$  orbital energy largely unperturbed. Strongly Lewis basic solvents (strong hydrogen-bond acceptors) were found to provide the greatest degree of  $d\pi(\text{Ru})$  orbital energy lowering. Accompanying the electrochemical effects are red shifts in the intervalence spectrum. Creutz and Chou concluded that the direction of the shift is consistent with a three-site delocalization mechanism involving a  $\pi^*$  orbital of the bridging ligand. Briefly, both the bonding and nonbonding molecular orbitals should be lowered in energy by ammine/solvent H-bonding. The effect should be greater, however, for the purely metal-derived nonbonding molecular orbital, than for the three-center (metal-bridge-metal) molecular orbital.

Similar effects have been observed based on double crown-ether encapsulation of the CT ion and a symmetrically substituted derivative, and similar conclusions have been reached concerning the applicability of a three-site delocalization mechanism.<sup>29</sup> In both the solvent and crown-encapsulation studies, however, the intervalence energy shifts are only about half as large as expected based on a simple  $d\pi(\text{Ru})-\pi^*(\text{pyrazine})-d\pi(\text{Ru})$  delocalization scheme. The additional involvement of pyrazine  $\pi$  orbitals could account for the smaller than expected environmental effects.

Raman scattering spectra, recorded in resonance with the intervalence transition, have been reported.<sup>13,30</sup> They reveal strong coupling of the transition to a totally symmetric vibration of the bridge,  $\nu_{6a}$ ; see below. This rules out a two-state delocalization scheme, but is consistent with a three-state scheme entailing light-induced transfer of charge symmetrically from the bridge to both metal centers. Additionally, the measurements show that only one Ru-N(pyrazine) vibration,

a symmetrical Ru-pyrazine-Ru stretch (Equation (4)), is coupled to the transition.<sup>30</sup> Given the oxidation-state sensitivity of the metal-ligand vibrations, two would be expected if the ion existed in valence-localized form.



## 2.60.6 DETAILED ELECTRONIC STRUCTURE

In addition to the intense intervalence band found at ca.  $5,800\text{ cm}^{-1}$ , the CT ion displays weaker electronic absorption bands at  $2,200\text{ cm}^{-1}$  and possibly  $3,500\text{ cm}^{-1}$ .<sup>31</sup> (Like the high-energy band, the band at  $2,200\text{ cm}^{-1}$  is narrow: the full-width at half-height is  $\sim 1,400\text{ cm}^{-1}$ .) The existence of one or two low-energy electronic bands points to the involvement of  $d\pi_{xy}(\text{Ru})$  and  $d\pi_{yz}(\text{Ru})$  orbitals; see Figure 5. In contrast to  $d\pi_{xz}$  orbitals, these are essentially unmixed and largely orthogonal to the bridging ligand's  $\pi$  and  $\pi^*$  orbitals. They can be viewed, therefore, as non-bonding orbitals that are localized on a single metal atom. Given this description, the low-energy intervalence transitions correspond to  $d-d$  transitions of an unusual kind: An electron is promoted from a localized  $d\pi_{xy}$  or  $d\pi_{yz}$  orbital to a delocalized  $d\pi_{xz}$ -derived orbital.<sup>12</sup> Thus, there is a net change in dipole moment and net (partial) metal-to-metal charge transfer; in the intervalence excited state, the hole created in the  $d\pi_{xy}$  or  $d\pi_{yz}$  orbital is confined to a single metal center. Because localized  $d\pi_{xy}$  and  $d\pi_{yz}$  orbitals exist on both metal centers, the low-energy intervalence transitions are doubly degenerate.

That the transitions are observed at all is likely a consequence of spin-orbit coupling and the resulting slight relaxation of orthogonality between the filled and half-filled  $d\pi(\text{Ru})$  orbitals. Indeed, when replacing ruthenium with osmium, having a much larger spin-orbit coupling coefficient, an extremely rich near- and mid-infrared absorption spectrum is observed, featuring several intense electronic transitions.<sup>32</sup>

## 2.60.7 ANOTHER PERSPECTIVE

Another view is that the CT ion exists in valence-localized form in the ground state but may be delocalized in one or more of the intervalence excited states. The available Stark data would appear to be incompatible with the proposed localized ground state to delocalized intervalence excited state transition, since the transition would require partial charge transfer and a significant ground-state/excited-state dipole moment difference. Demadis *et al.* have outlined how spin-orbit coupling, together with ligand-field asymmetry, could give rise to three intervalence bands, given a valence-localized ground state. Overlapping bands are identified at  $\sim 4,500$ ,  $6,300$ , and

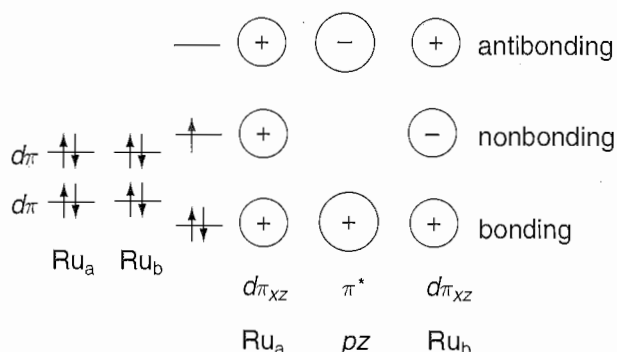


**Figure 5** Qualitative orbital diagram for the Creutz-Taube ion with inclusion of localized  $d\pi$  orbitals (two per metal center). The two low-energy intervalence transitions are ascribed to forbidden transitions involving promotion of an electron from a  $d\pi_{xy}$  or  $d\pi_{yz}$  orbital, confined to a single Ru, to the delocalized two-center nonbonding orbital.

7,300 cm<sup>-1</sup>. The weak bands found at ~2,200 and ~3,500 cm<sup>-1</sup> are assigned as Ru<sup>III</sup>-localized *d*-*d* transitions. The Demadis *et al.* description also accounts for the borderline behavior noted above. For example, residual IR intensity for an asymmetric pyrazine stretch can be explained by assuming weak localization. In the delocalized description, the residual intensity reflects environmental polarization of the ground electronic state (for example, by ion pairing), but the polarization is assumed to be too little to create a barrier on the ground potential energy surface. A summary description of the "orthodox" view would be that the CT ion is delocalized—but just barely, while a summary description of the alternative view would be that the CT is localized—but just barely.<sup>18</sup>

## 2.60.8 REFERENCES

1. Creutz, C.; Taube, H. *J. Am. Chem. Soc.* **1969**, *91*, 3988–3989.
2. Creutz, C.; Taube, H. *J. Am. Chem. Soc.* **1973**, *95*, 1086–1094.
3. Hush, N. S. *Trans. Faraday Soc.* **1961**, *57*, 557.
4. Hush, N. S. *Prog. Inorg. Chem.* **1967**, *8*, 391.
5. Tom, G. M.; Creutz, C.; Taube, H. *J. Am. Chem. Soc.* **1074**, *96*, 7827–7829.
6. Marcus, R. A. *J. Chem. Phys.* **1965**, *43*, 679.
7. Beattie, J. K.; Hush, N. S.; Taylor, P. R. *Inorg. Chem.* **1976**, *15*, 992–993.
8. Furholz, U.; Burgi, H. B.; Wagner, F. E.; Stebler, A.; Ammeter, J. H.; Krausz, E.; Clark, R. F. H.; Stead, M. J.; Ludi, A. *J. Am. Chem. Soc.* **1984**, *106*, 121–1239.
9. Piepho, S. B.; Krausz, E. R.; Schatz, P. N. *J. Am. Chem. Soc.* **1978**, *100*, 2996–3005.
10. Ondrechen, M. J.; Ellis, D. E.; Ratner, M. A. *Chem. Phys. Lett.* **1984**, *109*, 50–55.
11. Ondrechen, M. J.; Ko, J.; Zhang, L. T. *J. Am. Chem. Soc.* **1987**, *109*, 1666–1671, 1672–1676.
12. Piepho, S. B. *J. Am. Chem. Soc.* **1990**, *112*, 4197–4206.
13. Petrov, V.; Hupp, J. T.; Mottley, C. S.; Mann, L. C. *J. Am. Chem. Soc.* **1994**, *116*, 2171–2172.
14. Citrin, P. H. *J. Am. Chem. Soc.* **1973**, *95*, 6472–6473.
15. Hush, N. S. *Chem. Phys.* **1975**, *10*, 361–366.
16. Wishart, J.; Bino, A.; Taube, H. *Inorg. Chem.* **1986**, *25*, 3318–3222.
17. Best, S. P.; Clark, R. J. H.; McQueen, R. C. S.; Joss, S. J. *J. Am. Chem. Soc.* **1989**, *111*, 548–550.
18. Demadis, K. D.; Hartshorn, C. M.; Meyer, T. J. *Chem. Rev.* **2001**, *101*, 2655–2685, and references therein.
19. Ito, T.; Yamaguchi, T.; Kubiak, C. P. *Macromol. Symp.* **2000**, *156*, 269–275, and references therein.
20. Callahan, R. W.; Meyer, T. J. *Chem. Phys. Lett.* **1976**, *39*, 82–84.
21. Delarosa, R.; Chang, P. J.; Salaymeh, F.; Curtis, J. C. *Inorg. Chem.* **1985**, *24*, 4229–4231.
22. Oh, D. H.; Boxer, S. G. *J. Am. Chem. Soc.* **1990**, *112*, 8161–8162.
23. Oh, D. H.; Sano, M.; Boxer, S. J. *J. Am. Chem. Soc.* **1991**, *113*, 6880–6890.
24. Dong, Y. H.; Hupp, J. T.; Yoon, D. I. *J. Am. Chem. Soc.* **1993**, *115*, 4379–4380.
25. Petrov, V.; Williams, R. D.; Hupp, J. T. *Proceedings Of The XVth International Conference Of Raman Spectroscopy*, Asher, S. A., Stein, P., Eds.; John Wiley and Sons, New York, 1996; pp 768–771.
26. See, for example: Richardson, D. E.; Taube, H. *J. Am. Chem. Soc.* **1983**, *105*, 40–51.
27. Brunschwig, B. S.; Sutin, N. *Coord. Chem. Rev.* **1999**, *187*, 233–254.
28. Creutz, C.; Chou, M. H. *Inorg. Chem.* **1987**, *26*, 2995–3000.
29. Hupp, J. T.; Dong, Y. H. *Inorg. Chem.* **1994**, *33*, 4421–4424.
30. Lu, H.; Petrov, V.; Hupp, J. T. *Chem. Phys. Lett.* **1995**, *235*, 521–527.
31. Krausz, E. R.; Mau, A. W. H. *Inorg. Chem.* **1986**, *25*, 1484–1488.
32. Magnuson, R. H.; Lay, P. A.; Taube, H. *J. Am. Chem. Soc.* **1983**, *105*, 2507–2509.